J. Membrane Biol. 86, 27–36 (1985)

The Journal of
Membrane Biology

A Kinetic Analysis of the Electrogenic Pump of *Chara corallina*: III. Pump Activity during Action Potential

Uichiro Kishimoto, Yuko Takeuchi, Taka-aki Ohkawa, and Nobunori Kami-ike
Department of Biology, College of General Education, Osaka University, Toyonaka, 560 Japan

Summary. The current-voltage curve (I-V curve) of the *Chara* membrane was obtained by applying a slow ramp hyper- and depolarization by use of voltage clamp. By inhibiting the electrogenic pump with 50 μM DCCD (dicyclohexylcarbodiimide), the I-V curve approached a steady I-V curve within two hours, which gave the i_d-V curve of the passive diffusion channel. The i_p-V curve of the electrogenic pump channel was obtained by subtracting the latter from the former. The sigmoidal i_p-V curve could be simulated satisfactorily with a simple reaction kinetic model which assumes a stoichiometric ratio of 2. The emf of the pump (E_p) is given as the voltage at which the pump current changes its sign. The conductance of the pump (g_p) can be calculated as the chord conductance from the i_p-V curve, which is highly voltage dependent having a peak at a definite voltage. The changes of emf and conductance during excitation were determined by use of the current clamp ($I = 0$). Since the E_p and $g_p(V)$ are known, the changes, during excitation, of emf (E_d) and conductance (g_d) of the passive diffusion channel can be calculated. The marked increase of the membrane conductance and the large depolarization during the action potential are caused by the marked increase of the conductance of the passive diffusion channel and the large depolarization of its emf. The conductance of the electrogenic pump decreases to about half at the peak of action potential, while the pump current increases almost to a saturated level.

Key Words *Chara* · electrogenic pump · I-V curve · chord conductance · kinetic model · action potential

Introduction

The living cell keeps the internal ionic concentration quite different from the external medium. This unbalance of ionic distribution is maintained by active transport systems as well as by electrodiffusion. During excitation a large influx of Na^+ and a large efflux of K^+ are observed in the squid giant axon membrane (Hodgkin & Huxley, 1952). Similarly large effluxes of Cl^- and K^+ are observed during excitation of the excitable characean membranes (Gaffey & Mullins, 1958; Mullins, 1962; Hope & Findlay, 1964; Kishimoto, 1964, 1965; Hope & Walker, 1975). Furthermore, an increase in Ca^{2+} has also been suggested in relation to the sudden cessation of the cytoplasmic streaming during the action potential (Findlay & Hope, 1964; Beilby & Coster, 1979; Hayama et al., 1979; Williamson & Ashley, 1982; Kikuyama & Tazawa, 1983). The losses of chemical potentials for several ions during a single action potential of these giant cells may be negligibly small because of their large volume. However, the loss or gain of ions will be appreciable, if excitation is repeated many times. This is a particularly serious problem for the excitable cells of small size. Recovery of the original chemical potentials for lost ions with some means is essential. For this purpose activation of the active transport system is expected at some time during or after the action potential. Electrogenic ion pumps seem to be of greater importance in plants than in animals. Especially for plants living in fresh water, the electrogenic H^+-pump appears to be the primary active transport system (*see* review by Spanswick, 1981). The losses of chemical potentials for these ions need to be recovered as soon as possible. The most likely candidate for this recovery mechanism in *Chara* is the activation of the electrogenic H^+-pump. Therefore, it is important to investigate the temporal change of activity of the H^+-pump during the action potential.

In *Chara*, the electrogenic H^+-pump hyperpolarizes the membrane potential by about 100 mV beyond the level of the electrodiffusion potential (Kitasato, 1968). The current-voltage curve (i_p-V curve) of the electrogenic pump is sigmoidal in a normal pH range (6.5 to 7.5) and could be simulated satisfactorily with a kinetic reaction model assuming the cyclic changes of H^+-ATPase in the plasma membrane (Kishimoto et al., 1984; Takeuchi et al., 1985). This analysis assigns the electrogenic pump a voltage-independent reversal potential (E_p) and a voltage-dependent conductance (g_p), which has a

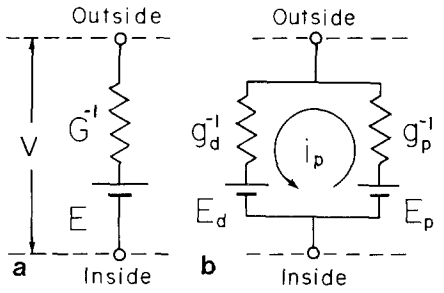

Fig. 1. (*a*) A simplified Thévenin model for the *Chara* membrane. (*b*) Parallel circuit model for the *Chara* membrane. The passive diffusion channel as well as the electrogenic pump channel has its own conductance in series with the respective emf

single peak. On the other hand, changes of emf and conductance of the *Chara* membrane during excitation can be determined precisely by use of a current-clamp method (Kishimoto et al., 1982). Since g_p of the pump is known as a function of voltage, changes during excitation of conductance and emf of the passive channel as well as g_p of the pump can be evaluated.

Materials and Methods

Giant internodes of *Chara corallina* were used throughout the present experiments. The internodes, which averaged 0.7 mm in diameter and 6 cm in length, were isolated from adjacent cells. Next, the internodes were kept in artificial pond water (APW) for at least two days with a photoperiod of 12 hr light (*ca.* 2000 lx) and 12 hr dark. The APW contained (in mM): 0.5 KCl, 0.2 NaCl, 0.1 $Ca(NO_3)_2$ and 0.1 $Mg(NO_3)_2$, and the pH was buffered at 7 with 2 mM TES (N-Tris(hydroxymethyl)methyl-2-aminoethane sulfonic acid). The external APW was perfused at a constant rate of about 1 liter/hr. Temperature of the solution was set at about 20°C with a thermoelectric regulator (Sharp, TE-12K) and was monitored with a thermistor. The external pH was monitored with a glass pH electrode.

The details of the voltage clamp and the current clamp were the same as described previously (Kishimoto et al., 1980, 1981, 1982). The space constant of the internode we used was about 3 cm at rest and 6 mm at the peak of excitation. As a compromise for accuracy in the surface area estimation and in the spatial uniformity of the voltage clamping, we chose the length of the measuring region as 6 mm.

We assume that the *Chara* membrane has two independent ionic pathways, i.e., one being the passive diffusion channel and another the electrogenic pump (Fig. 1*b*). The *I-V* curve was obtained by applying a ramp hyperpolarization first and a ramp depolarization next under the voltage clamp. The ramp rate 100 mV/30 sec was found to be slow enough to give a steady *I-V* relation (Kishimoto et al., 1984). Later, a similar *I-V* curve was obtained after inhibiting the electrogenic pump with 50 μM DCCD (dicyclohexylcarbodiimide). The latter corresponds to the i_d-*V* curve of the passive diffusion channel (Kishimoto et al., 1984). The i_p-*V* curve of the electrogenic pump was obtained by subtracting the latter from the former. The conductance of the *Chara* membrane was determined following an improved method under the current clamp ($I = 0$) condition (Kishimoto et al., 1982). After A/D conversion of the current data, together with the voltage and trigger pulse with a Data Acquisition System (MDAS 8D, Datel), they were recorded with a floppy disk system (YE DATA). The current and voltage data thus digitized served for later computations.

The experimental sigmoidal i_p-*V* curves could be generally simulated successfully with Eq. (7) below, which assumes cyclic changes of the H^+-ATPase. Four unknown parameters, i.e., A_1, A_2, A_3 and A_4 were determined with a program of successive approximation to find the least sum of squared errors (Powell, 1965; Kotani, 1979). Actual computation was carried out through a terminal microcomputer (PC9801E, NEC) by MELCOM (Mitsubishi, a main frame computer) in the Computer Center of Osaka University. Rate constants in Fig. 2 were calculated from A_1, A_2, A_3 and A_4. By using these four parameters, the reconstructed i_p-*V* curve (full lines in Figs. 3 and 4), with corresponding actual data (shown with symbols in Figs. 3 and 4), were displayed with an *X-Y* plotter (Watanabe, WX4671). The computed chord conductance of the electrogenic pump is shown in these figures with dotted lines.

The data in this report are not the average on different internodes, but on a single internode. We noticed that there was some variation in the activity of the electrogenic pump among internodes. However, the type of change in activity during the action potential was very similar among ten internodes tested.

Results

DCCD is known as a specific blocker of the F_o, F_1-ATPase of mitochondrial inner membrane and also of the thylakoid in chloroplasts. It binds to one of the subunits, resulting in blockage of the H^+ flux through the H^+-channel portion of the ATPase. Actually the internal ATP level decreased to almost one-third of the original level by treating the *Chara* internode with 50 μM DCCD (Keifer & Spanswick, 1979; Takeuchi & Kishimoto, 1983). DCCD was dissolved in the APW and pH was adjusted to 7 with TES. The DCCD solution was also perfused externally at a constant speed of about 1 liter/hr.

During inhibition of the electrogenic pump with DCCD, the *I-V* curve moved by about 100 mV (depolarization) along the voltage axis, reducing its slope (Kishimoto et al., 1984). About 150 min after application of DCCD in the dark, the *I-V* curve reached a steady state. This steady state lasted for about an hour. At this stage the *V* for $I = 0$ was about -125 mV, which is thought to be the E_d of the passive diffusion channel. The *Chara* is excitable at this stage, having almost the same peak level of action potential. We adopted this *I-V* curve as the i_d-*V* curve of the passive diffusion channel. The i_p-*V* curve of the electrogenic pump could be obtained by subtracting the i_d-*V* curve from the *I-V* curve. The details were reported previously (Kishimoto et al., 1984).

Consecutive Reaction Scheme for the H^+-Pump

We need a kinetic model to analyze the voltage-dependent pump characteristics. Several kinetic models assuming the cyclic changes of enzyme intermediates have been proposed by several authors (Läuger, 1979, 1980; Hansen et al., 1981; Steinmetz & Anderson, 1982; Chapman et al., 1983; Oosawa & Hayashi, 1983; Beilby, 1984; Kishimoto et al., 1984). In a previous report (Kishimoto et al., 1984), we adopted a kinetic model which assumed a cyclic change of five states of H^+-ATPase in the plasmalemma of the *Chara* (Fig. 2*b*). In this model we had four rate constants and three equilibrium constants. We could decide four parameters which determine the shape of the experimental i_p-V curve of the pump with the aid of computer simulation. Therefore, we needed several assumptions in order to discuss the changes of rate constants and equilibrium constants with the change in physiological condition. An alternative is to adopt a lumped 2-state model (Fig. 2*a*) which was introduced by Hansen and co-workers (1981). In this model the voltage-dependent step is expressed with two rate constants, i.e., k_{12} (forward) and k_{21} (backward). These are voltage dependent. On the other hand, the voltage-independent step is expressed with two rate constants, i.e., κ_{21} (forward) and κ_{12} (backward). These are not voltage dependent. In this model we have only four rate constants. Therefore, it is possible to evaluate all of these rate constants from four parameters which are determined from simulation of the experimental i_p-V curve.

We assume that efflux or influx of H^+ occurs by the steady cyclic change of enzyme intermediates either clockwise or counter-clockwise. The rate of transition from E_1 into E_2 in the voltage-dependent step is given by,

$$f_{12} = k_{12}E_1 - k_{21}E_2 \tag{1}$$

where E_1 and E_2 are densities of E_1 and E_2, respectively. These abbreviations are used hereafter. For further simplicity, a symmetry in the energy barriers for the forward and backward transition is also assumed (Läuger, 1979). Then,

$$k_{12} = k^o_{12}\exp(mFV/2RT);\ k_{21} = k^o_{21}\exp(-mFV/2RT) \tag{2}$$

$$f_{12} = k^o_{12}\exp(mFV/2RT)E_1 - k^o_{21}\exp(-mFV/2RT)E_2 \tag{3}$$

where m is the number of charge moved during this transition. In our model (Fig. 2*a*) m is assumed to be equal to the stoichiometric ratio. R, F and T have their usual meanings.

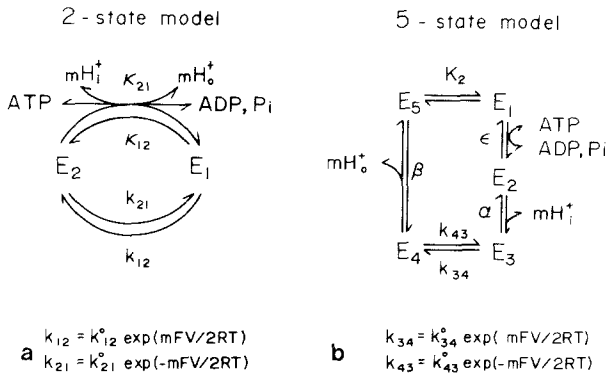

Fig. 2. Kinetic schemes for the vectorial H^+-ATPase of the electrogenic pump of the *Chara* membrane. (*a*) A lumped 2-state model having four rate constants. k_{12} and k_{21} are the rate constants for the voltage-dependent (electrogenic) step, while κ_{21} and κ_{12} are those for the voltage-independent step. (*b*) A previous model which assumes a cyclic change of five states of H^+-ATPase in the plasmalemma (Kishimoto et al., 1984). In this model coupling with ATP-hydrolysis, incorporation and release of m H^+ are expressed with equilibrium constants. The forward and backward rate constants in a step $E_5 \rightleftharpoons E_1$ are assumed to be the same. All these reactions are assumed to be voltage independent. These are lumped together and are expressed with two rate constants, κ_{21} and κ_{12} in the 2-state model in *a*. Only the step $E_3 \rightleftharpoons E_4$ is assumed to be charge carrying and electrogenic in *b*

The rate of transition of the enzyme from E_2 into E_1 in the voltage-independent step is given by,

$$f_{21} = \kappa_{21}[\mathrm{ATP}][\mathrm{H}_i]^m E_2 - \kappa_{12}[\mathrm{ADP}][\mathrm{P}_i][\mathrm{H}_o]^m E_1. \tag{4}$$

At the steady state, f_{12} is equal to f_{21}. Total amount of enzyme (E_o) is assumed to remain unchanged. By use of these two conditions the amount of enzyme intermediate can be calculated as follows;

$$E_1 = (k^o_{21}/D + \kappa_{21}[\mathrm{ATP}][\mathrm{H}_i]^m)E_o/W \tag{5}$$

$$E_2 = (k^o_{12}D + \kappa_{12}[\mathrm{ADP}][\mathrm{P}_i][\mathrm{H}_o]^m)E_o/W \tag{6}$$

where $D = \exp(mFV/2RT)$ and

$$W = k^o_{12}\,D + k^o_{21}/D + \kappa_{21}[\mathrm{ATP}][\mathrm{H}_i]^m + \kappa_{12}[\mathrm{ADP}][\mathrm{P}_i][\mathrm{H}_o]^m.$$

The current carried by H^+, i.e., i_p (pump current) is proportional to f_{12} ($=f_{21}$). Then, i_p can be calculated with Eqs. (3) through (6).

$$i_p = \frac{[\exp(mFV/2RT) - A_1\exp(-mFV/2RT)]A_4}{\exp(mFV/2RT) + A_2\exp(-mFV/2RT) + A_3} \tag{7}$$

where

$$A_1 = (k^o_{21}/k^o_{12})(\kappa_{12}/\kappa_{21})([\mathrm{ADP}][\mathrm{P}_i]/[\mathrm{ATP}])([\mathrm{H}_o]/[\mathrm{H}_i])^m \tag{8}$$

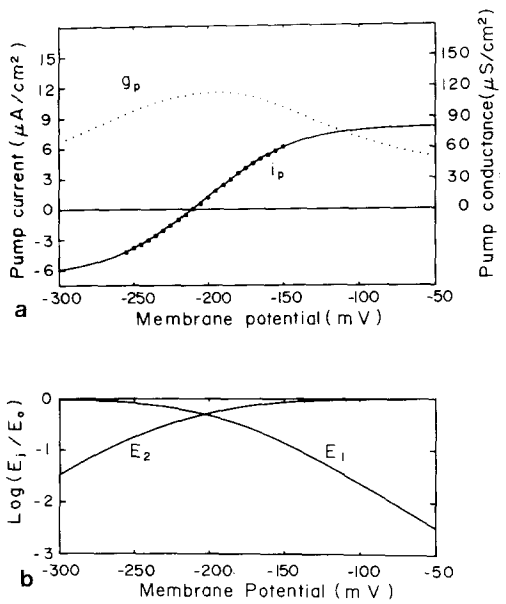

Fig. 3. (*a*) The current-voltage curve (i_p-V curve) of the electrogenic pump before DCCD poisoning. The symbols are the experimental i_p-V data which are plotted at 5-mV intervals. The full line is the simulated curve using Eq. (7) in the text. The dotted curve is the chord conductance of the electrogenic pump which was calculated with Eq. (17) in the text. (*b*) Changes of fraction of each enzyme intermediate state with voltage. These were calculated with Eqs. (5) and (6)

$$A_2 = k_{21}^o/k_{12}^o \tag{9}$$

$$A_3 = (\kappa_{21}[\mathrm{ATP}][\mathrm{H}_i]^m + \kappa_{12}[\mathrm{ADP}][\mathrm{P_i}][\mathrm{H}_o]^m)/k_{12}^o \tag{10}$$

$$A_4 = mFE_o\kappa_{21}[\mathrm{ATP}][\mathrm{H}_i]^m. \tag{11}$$

The functional shape of the pump current in this lumped 2-state model is the same as that in the previous 5-state model (Kishimoto et al., 1984). From these four equations, the four rate constants in Fig. 2*a* can be calculated.

$$\kappa_{21} = A_4/(mFE_o[\mathrm{ATP}][\mathrm{H}_i]^m) \tag{12}$$

$$\kappa_{12} = \kappa_{21}(A_1/A_2)([\mathrm{ATP}]/[\mathrm{ADP}][\mathrm{P_i}])([\mathrm{H}_i]/[\mathrm{H}_o])^m \tag{13}$$

$$k_{12}^o = (\kappa_{21}[\mathrm{ATP}][\mathrm{H}_i]^m + \kappa_{12}[\mathrm{ADP}][\mathrm{P_i}][\mathrm{H}_o]^m)/A_3;\ k_{12} = k_{12}^o\, D \tag{14}$$

$$k_{21}^o = k_{12}^o A_2;\ k_{21} = k_{21}^o/D. \tag{15}$$

E_p can be calculated as the voltage where $i_p = 0$.

$$E_p = RT/(mF)\ \ln(A_1) = RT/(mF)[\ln(k_{21}^o/k_{12}^o) + \ln(\kappa_{12}/\kappa_{21}) + \ln([\mathrm{ADP}][\mathrm{P_i}]/[\mathrm{ATP}]) + m\ \ln([\mathrm{H}_o]/[\mathrm{H}_i])]. \tag{16}$$

The conductance g_p of the electrogenic pump is given as a chord conductance. That is,

$$g_p = i_p/(V - E_p). \tag{17}$$

The slope of the i_p-V curve has been adopted, on not a few occasions, as the conductance of the electrogenic pump. If this were the case, such a conductance would be zero for a large depolarization or for a large hyperpolarization. The pump is acting as a constant current source in these voltage ranges. However, it is a paradox for the conductance in a finite voltage range to be zero irrespective of a non-zero value of i_p. In our present model (Fig. 1*b*), g_p should be the chord conductance and the size of g_p is to be calculated with Eq. (17).

The real i_p-V curve can be simulated satisfactorily by Eq. (7) with the aid of a computer program of successive approximation to find the least sum of squared errors (Powell, 1965; Kotani, 1979) and values of A_1, A_2, A_3 and A_4 are determined. Thus, i_p and g_p at any voltage can be calculated with Eqs. (7) and (17).

It is important to estimate the speed of cyclic changes of enzyme intermediate in our kinetic model (e.g., Hansen et al., 1983). The rate of change in density of E_2 is expressed as follows

$$dE_2/dt = k_{12}E_1 + \kappa_{12}[\mathrm{ADP}][\mathrm{P_i}][\mathrm{H}_o]^m E_1 - k_{21}E_2 - \kappa_{21}[\mathrm{ATP}][\mathrm{H}_i]^m E_2.$$

Since $E_1 + E_2 = E_o$,

$$dE_2/dt = (k_{12} + \kappa_{12}[\mathrm{ADP}][\mathrm{P_i}][\mathrm{H}_o]^m)E_o - (k_{12} + k_{21} + \kappa_{12}[\mathrm{ADP}][\mathrm{P_i}][\mathrm{H}_o]^m + \kappa_{21}[\mathrm{ATP}][\mathrm{H}_i]^m)E_2.$$

Thus,

$$E_2 = (k_{12} + \kappa_{12}[\mathrm{ADP}][\mathrm{P_i}][\mathrm{H}_o]^m)E_o[1 - \exp(-t/\tau)] + E_{2,\mathrm{initial}}\exp(-t/\tau)$$

$$\tau = 1/(k_{12} + k_{21} + \kappa_{21}[\mathrm{ATP}][\mathrm{H}_i]^m + \kappa_{12}[\mathrm{ADP}][\mathrm{P_i}][\mathrm{H}_o]^m)$$

where τ is the time constant for the change. Substitution of the four rate constants which are determined from the experimental i_p-V curve (Fig. 8*b*) gives us very small value ($<10^{-6}$ sec) for the time constant before as well as 110 min after application of DCCD. In other words, the cyclic change of the enzyme intermediate in the *Chara* membrane is generally very fast. Therefore, our assumption of steady cyclic changes of enzyme intermediates dur-

ing the voltage span as well as during an action potential has experimental grounds in the case of the *Chara* membrane.

Change of i_p-V Relation During DCCD Poisoning

Two sets of i_p-V curves and g_p-V curves, before and 110 min after application of 50 μM DCCD, are shown in Figs. 3*a* and 4*a*. The i_p-V curve is generally sigmoidal and g_p has a single peak. The experimental i_p are shown with symbols at 5-mV intervals. The full line for i_p-V and dotted line for g_p are the simulated and calculated curves, respectively. The general tendencies are decreases of i_p and g_p with the progress of DCCD poisoning. The emf of the electrogenic pump depolarized only by about 10 mV in the light. These results are almost the same as reported previously (Kishimoto et al., 1984). The changes in fractions of enzyme intermediates are also shown in Figs. 3*b* and 4*b*. The general pattern of the change of enzyme intermediate with depolarization are the decrease of E_1, and the increase of E_2.

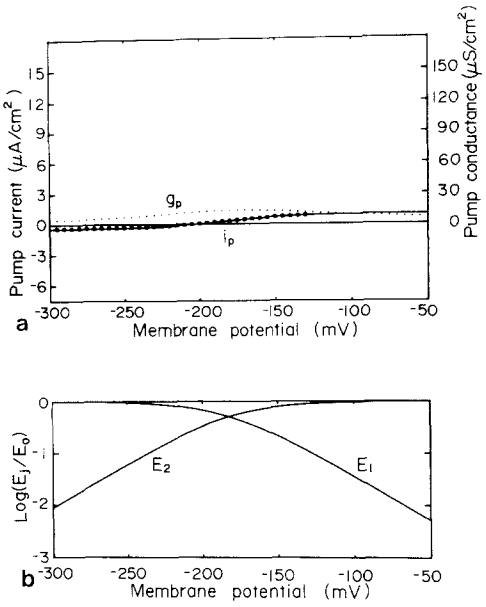

Fig. 4. (*a*) The i_p-V curve of the electrogenic pump about 110 min after application of 50 μM DCCD in the light. The symbols are the recorded i_p-V data which are plotted at 5-mV intervals. At this stage the inhibition of the pump progressed greatly but it was not complete yet. The full line is the simulated curve. The dotted curve is the chord conductance of the electrogenic pump. (*b*) Changes of fraction of each enzyme intermediate state with voltage

Changes of emf's, Conductances, Pump Current and Enzyme Intermediates During Action Potential

In our parallel circuit model (Fig. 1*b*) the measured conductance G (Fig. 1*a*) is the sum of g_d and g_p.

$$G = g_d + g_p \tag{18}$$

and the measured emf (E) is the weighted average of two emf's, i.e., E_d and E_p. Here the weights are the conductances of each channel, i.e., g_d and g_p.

$$E = (g_d E_d + g_p E_p)/G. \tag{19}$$

Under the condition where $I = 0$, i_p should flow back into the cell through the passive diffusion channel. Therefore,

$$i_p = g_p(E - E_p) = g_d(E - E_d). \tag{20}$$

Both conductances are generally voltage dependent.

The time course of action potential of *Chara* membrane is generally slow. However, the capacity current rises to the order of 1μA/cm^2 in its rising phase. In the later period the capacity current is negligible. In other words, the sum of total ionic currents during action potential is zero except for the initial rising phase. Therefore, we can suppose that the action potential of the *Chara* membrane is approximately the locus of zero total ionic current. The conductance G and its change during the action potential can be determined precisely from the analysis of the voltage responses caused by small square current pulses which are superimposed intermittently under the current clamp ($I = 0$) condition (Kishimoto et al., 1982). On the other hand, the conductance (g_p) of the electrogenic pump can be evaluated as a function of voltage from the i_p-V curve at each stage of DCCD poisoning (Figs. 3*a* and 4*a*). Knowing g_p as a function of voltage, it is possible to calculate changes of g_d and E_d of the passive diffusion channel and the pump current during a single action potential with Eqs. (18)–(20). It is also possible to calculate the changes of each enzyme intermediate during the action potential with Eqs. (5), (6), and (12)–(15). Those results are shown in Figs. 5 and 6.

The marked increase of membrane conductance G is mainly caused by the marked increase of g_d of the passive diffusion channel (Figs. 5*b* and 6*b*). The extent of increase of g_d decreases with the progress of DCCD poisoning. On the other hand, conductance of the electrogenic pump (g_p) decreases to

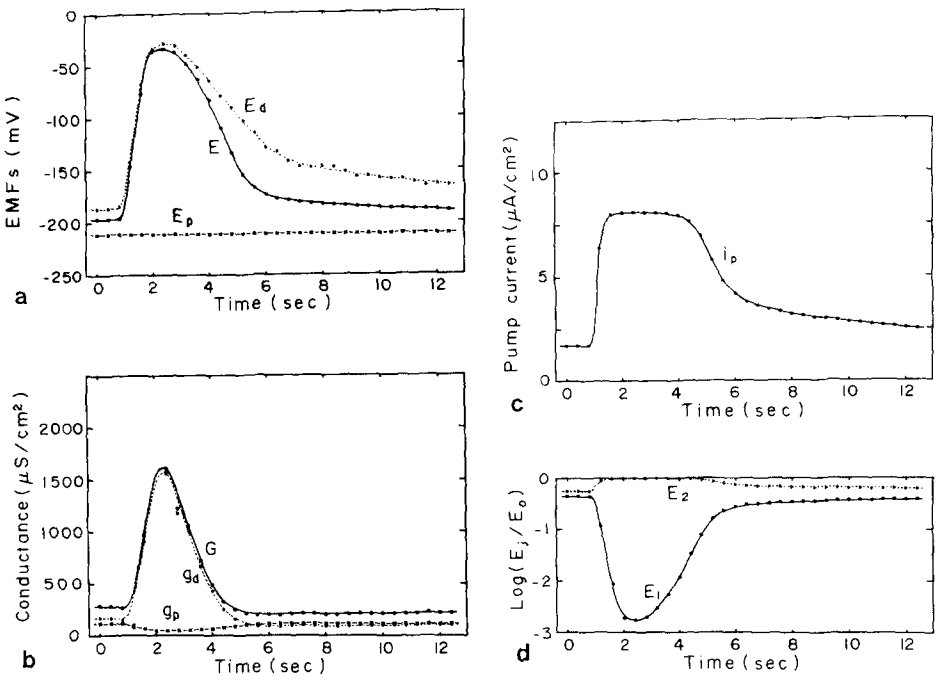

Fig. 5. Changes of electric parameters during the action potential before DCCD poisoning. (*a*) Changes of emf's under the current-clamp condition ($I = 0$). E is the recorded action potential, E_d the calculated emf change of the passive diffusion channel. E_p of the electrogenic pump is voltage independent. (*b*) G is the measured membrane conductance, g_d the conductance of the passive diffusion channel and g_p the chord conductance of the electrogenic pump during the action potential. Note that g_d increases markedly, while g_p decreases to almost half during the action potential. (*c*) The pump current i_p increases to a saturated level at around the peak of the action potential. (*d*) Changes of fraction of each enzyme intermediate state during the action potential. These changes are simply caused by the change in membrane potential

half temporarily during the action potential. This is also expected from the sigmoidal i_p-V curve in Figs. 3*a* and 4*a*. That is, the g_p at large depolarization is about half of that at the resting potential.

Changes of E_d of the passive diffusion channel are almost in parallel with those of E (Figs. 5*a* and 6*a*). This is caused by the marked increase of g_d. It is worth noting that the peak of E_d during the action potential does not change appreciably by DCCD poisoning. DCCD seems to have no appreciable influence on the passive channel. The emf of the electrogenic pump (E_p) is assumed to be unchanged during the action potential. This is expected in our kinetic model (Eq. 16).

The pump current i_p increases to a saturated level at around the peak of the action potential and later it decreases slowly. The i_p and the extent of its increase during action potential decrease with the progress of DCCD poisoning (Figs. 5*c* and 6*c*). It is worth noting that the tail of the action potential, the time courses of recoveries of the pump current and of the fractions of the enzyme intermediates prolong considerably with the progress of DCCD poisoning (Fig. 6). In other words, this current which flows inwardly through the passive channel is quite large before inhibition of the electrogenic pump occurs, and seems to help inactivate the excitatory mechanism.

During the action potential, E_2 increases while E_1 decreases (Figs. 5*d* and 6*d*). These changes in the fractions of enzyme intermediates are caused by the change in membrane potential (Figs. 3*b* and 4*b*).

Discussion

The current-voltage curve of the electrogenic pump channel in a normal pH range between 6.5 and 7.5 is sigmoidal and could be simulated with a kinetic reaction model which assumes the cyclic changes of the H^+-ATPase (Takeuchi et al., 1985). The reversal potential or the emf (E_p) of the electrogenic pump is about −220 mV at pH 7. The level E_p hyperpolarizes with a slope of 40 to 50 mV/pH for the increase of external pH. Therefore, it is highly likely that the electrogenic pump of the *Chara* membrane is a 2 H^+/1 ATP type proton pump. On the other hand, Beilby (1984) and Smith (1984) suppose that the stoichiometric ratio of the proton pump in *Chara* plasmalemma may be 1. We tried to find out

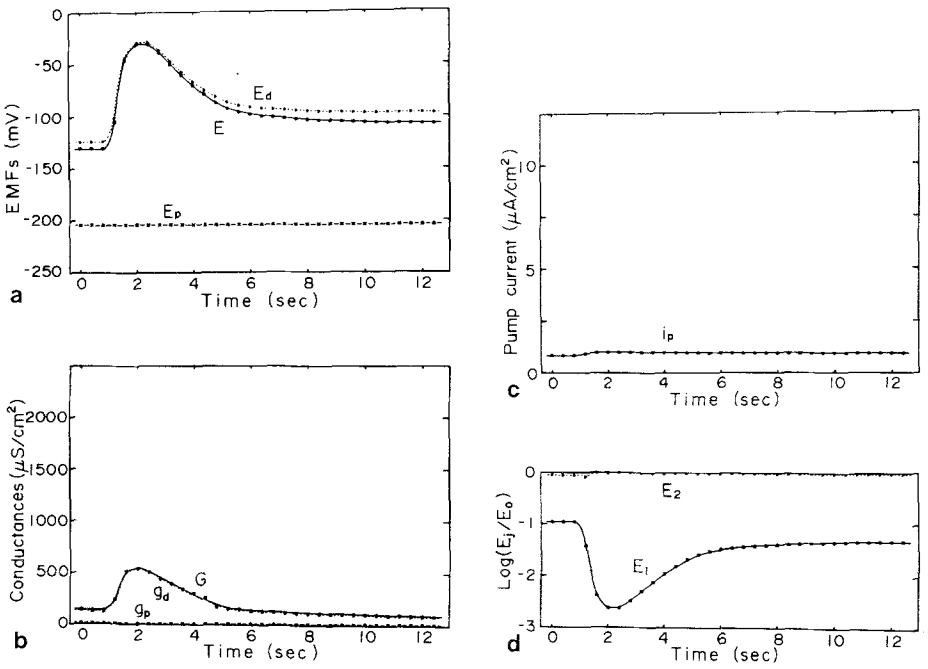

Fig. 6. Changes of electric parameters during the action potential about 110 min after application of 50 μM DCCD. (*a*) Changes of emf's under the current-clamp condition ($I = 0$). E is the recorded action potential, E_d the calculated emf change of the passive diffusion channel. E_p of the electrogenic pump is voltage independent. (*b*) G is the measured membrane conductance, g_d the conductance of the passive diffusion channel and g_p the conductance of the electrogenic pump during the action potential. Note that g_d increases markedly, while g_p decreases to almost half during the action potential. (*c*) The pump current i_p increases to a saturated level at around the peak of action potential. (*d*) Changes of fraction of each enzyme intermediate state during the action potential. These changes are simply caused by the change in membrane potential

the most suitable value for the stoichiometry (m) with the aid of computer simulation. Every time, we found m was close to 2 under a normal experimental condition ($pH_o = 7$ and in the light). Therefore, we adopt a value of 2 for m in the present analysis. We also found that the shape of the current-voltage curve deformed to some extent, if we include a larger voltage range. Moreover, we noticed that E_p also changed to some extent for the large voltage change (Ohkawa et al., *unpublished*), which suggested a possibility of some change in internal pH near the plasmalemma, or changes in either one or all of four rate constants (Eq. 16) under this condition. Such a change in E_p during a voltage span would change the shape of the i_p-V curve. This is the main reason why we chose a comparatively limited voltage range in our voltage span.

On the other hand, the conductance of the electrogenic pump, which is calculated as the chord conductance from the i_p-V curve, is highly voltage dependent, having a peak at around the resting potential level. Therefore, the same amount of current as i_p flows inward through the passive diffusion channel, causing hyperpolarization of the *Chara* membrane at the resting state. The amount of this current, which has been supposed to express the activity of the pump, depends on the emf's and conductances of active as well as those of passive channels (Eqs. 19 and 20).

Changes in conductance and emf of the *Chara* membrane during the action potential are caused mainly by the marked increase of conductance (g_d) and the large depolarization of the passive diffusion channel (Figs. 5 and 6). This indicates that excitation of the *Chara* membrane is an event which occurs in the passive diffusion channel.

The chord conductance (g_p) of the electrogenic pump decreased by about half at the peak of action potential (Figs. 5*b* and 6*b*). This is demonstrated clearly with the voltage-dependent characteristic of the chord conductance (dotted curves in Figs. 3*a* and 4*a*). In other words, g_p is close to its peak at the resting state voltage, while it decreases markedly for a large depolarization. This can also be expected from the sigmoidal shape of the i_p-V curve (full lines in Figs. 3*a* and 4*a*). Nevertheless, the pump current (i_p) increases markedly, almost to a saturation level, at around the peak of action potential (Figs. 5*c* and 6*c*). The same amount of current needs to flow inward through the passive diffusion channel in

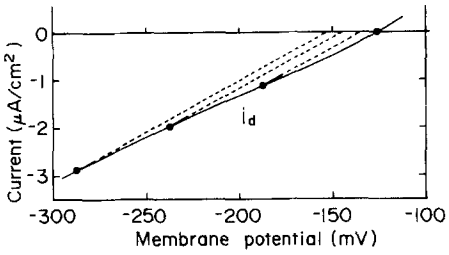

Fig. 7. The current-voltage curve (i_d-V curve) of the passive diffusion channel, which was obtained under the ramp voltage-clamp condition on another *Chara* internode at the latest stage of inhibition of the pump by 50 μM DCCD. During this ramp voltage clamp small square voltage pulses were superimposed to see the change of the instantaneous Δi_d-Δv relation. Only the region of hyperpolarization is shown here. The slope of this Δi_d-Δv line gives the conductance and the extrapolation of this line (shown with dotted lines) to the voltage axis gives the emf of the passive channel at the respective voltage. At voltage close to E_d where $i_d = 0$ the slope of the line is equal to the slope of the i_d-V curve and the emf is equal to E_d. However, it it worth noting that the slope becomes larger than the slope of the i_d-V curve with hyperpolarization of the membrane and that the emf of the passive diffusion channel hyperpolarizes. However, the extent of this hyperpolarization of emf of the passive channel saturates (about 40 mV, *data not shown*)

Chara for the electroneutrality. Therefore, the marked increase of i_p may appear to limit the voltage excursion during the action potential. However, this extent is actually very small because of marked increase of g_d at the peak of the action potential (Figs. 5*b* and 6*b*). With the progress of DCCD poisoning, both g_p and i_p and also the extent of their increases during action potential decrease (Figs. 3*a*, 4*a*, 5*c* and 6*c*). However, it is worth noting that the peak level of E_d of the passive diffusion channel at around the peak of action potential remains almost unchanged during DCCD poisoning. This seems to suggest that the excitatory mechanism of the passive diffusion channel was not affected directly by DCCD. In practice, the extent of increase of g_d during action potential becomes less with the progress of DCCD poisoning. This is probably caused by the voltage-dependent activation and inactivation of the passive excitatory channels. The details remain to be checked.

At the later stage of DCCD poisoning E_d is about -125 mV (Fig. 6*a*). On the other hand, the level of E_d before excitation is not necessarily close to about -125 mV in Fig. 5*a*, but is at a somewhat more hyperpolarized level. This is caused by the voltage dependence of g_d as well as of E_d. If we superimpose short square voltage pulses intermittently on the slow ramp hyperpolarization, we obtain the instantaneous Δi_d-Δv relation at corresponding voltages (Fig. 7). The extrapolation of these Δi_d-Δv curves to the voltage axis gives the emf's of the passive diffusion channel at respective voltage. These emf's are not necessarily equal to the E_d at $i_d = 0$, but shift toward hyperpolarized level in proportion to the extent of externally applied hyperpolarization. This is the reason why the E_d at rest before DCCD poisoning is at a somewhat hyperpolarized level. Also, the slope of each instantaneous Δi_d-Δv relation gives the instantaneous chord conductance at respective voltages and is not necessarily equal to the slope of the i_d-V curve. This instantaneous chord conductance is equal to the slope of the i_d-V curve only at the voltage where $i_d = 0$.

Changes of four parameters (A_1, A_2, A_3 and A_4), during inhibition of the electrogenic pump of a single internode, by 50 μM DCCD are shown in Fig. 8*a*. These parameters characterize the shape of the i_p-V curve. Typical features of the DCCD poisoning are marked increases of A_1 and A_2, a marked decrease of A_4 and a slight change of A_3. This is the result of simulation of the experimental i_p-V curve and does not change with the kinetic model we adopt.

Changes of four rate constants (k^o_{12}, k^o_{21}, κ_{21} and κ_{12}) in the present lumped 2-state model are shown in Fig. 8*b*. With the progress of inhibition of the pump by 50 μM DCCD, k^o_{12}, κ_{21} and κ_{12} decrease markedly, while k^o_{21} shows only a slight change. In a previous report (Kishimoto et al., 1984) we described the changes of kinetic parameters in the 5-state model (Fig. 2*b*) during inhibition of the electrogenic pump. The equilibrium constants (ε, α and β) and two rate constants (k^o_{51} and k^o_{15}) in the former 5-state model are lumped together into the two rate constants (κ_{21} and κ_{12}) in the 2-state model. The values of these kinetic parameters depend on the model we choose. Our present results are the marked decreased of forward rate constant in the electrogenic step and marked decreases of two rate constants in the nonelectrogenic step. These are substantially in common with those reported previously.

The conductance of the tonoplast of *Chara* internode is generally about 10 times as large as that of the plasmalemma and the membrane potential at the tonoplast is about 10 mV, the cytoplasm being negative to the vacuole (Findlay & Hope, 1964; Hope & Walker, 1975). We have reconfirmed these results. They also demonstrated that the tonoplast potential showed a slow transient hyperpolarization and increase in its conductance at the peak of action potential. At present we have no quantitative data on the pump activity at the tonoplast of the *Chara*. However, the large conductance and small membrane potential at the tonoplast suggest that the electrogenicity of the pump, if any, at the tonoplast

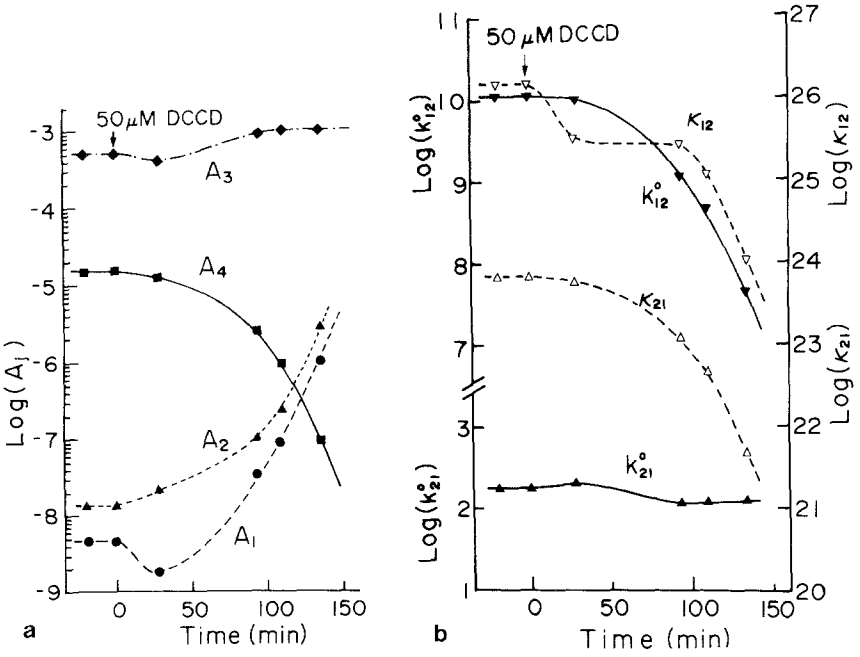

Fig. 8. (*a*) Changes of four parameters (A_1, A_2, A_3 and A_4), which characterize the shape of the experimental i_p-V curve of the electrogenic pump, during inhibition by 50 μM DCCD. (*b*) Changes of four rate constants in the 2-state model (Fig. 2*a*) for the pump during inhibition by 50 μM DCCD. The data shown in Figs. 3 and 5 were obtained at zero time in these figures, while those in Figs. 4 and 6 were obtained about 110 min after application of DCCD

should be very small. Thus, we can regard safely the i_p-V curve shown in this report as mainly that of the plasmalemma.

We may underestimate g_d by about 10% at rest, since we neglected the contribution from the tonoplast in the present report. Moreover, the increase of g_d at the peak of action potential may be a few times as large as that reported here. Therefore, g_d and G may be larger than those shown in Figs. 5*b* and 6*b*. Nevertheless, the features of the electrogenic pump such as decrease of g_p and increase of i_p during an action potential remain unaffected.

Smith and Beilby (1983) showed a long-lasting yet transient decrease of the membrane conductance after an action potential in *Chara*. They speculated this first due to inhibition of the electrogenic pump during and after an action potential. This notion seems to be discarded later by Beilby (1984) by the measurements of g_p as a function of voltage. Our data are on the changes in the g_p of the electrogenic pump and the pump current during a single action potential. Actually the i_p-V curve itself of the pump is not affected at all during the action potential. What occurs in the pump is a decrease in g_p and an increase in i_p which are simply results of the shift of the voltage in the i_p-V curve. We suppose the change in conductance after the action potential (Smith & Beilby, 1983) is something else, which we have not examined yet.

The marked increase of the pump current suggests, in our kinetic model, that a temporary large consumption of ATP may occur during the action potential. This remains to be checked experimentally.

We are indebted to Ms. Y. Saegusa for her excellent secretarial assistance. This work was supported by a Research Grant from the Ministry of Education, Science and Culture of Japan. A preliminary communication on the same topics is in press in *Biomed. Res.* (Tokyo).

References

Beilby, M.J. 1984. Current-voltage characteristics of the proton pump at *Chara* plasmalemma: I. pH dependence. *J. Membrane Biol.* **81:**113–125

Beilby, M.J., Coster, H.G.L. 1979. The action potential in *Chara corallina*. II. Two activation-inactivation transients in voltage clamps of the plasmalemma. *Aust. J. Plant Physiol.* **6:**323–335

Chapman, J.B., Johnson, E.A., Kootsey, J.M. 1983. Electrical and biochemical properties of an enzyme model of the sodium pump. *J. Membrane Biol.* **74:**139–153

Findlay, G.P., Hope, A.B. 1964. Ionic relations of cells of *Chara australis*. VII. The separate electrical characteristics of the plasmalemma and tonoplast. *Aust. J. Biol. Sci.* **17:**62–77

Gaffey, C.T., Mullins, L.J. 1958. Ion fluxes during the action potential in *Chara*. *J. Physiol. (London)* **144:**505–524

Hansen, U.-P., Gradmann, D., Sanders, D., Slayman, C.L. 1981. Interpretation of current-voltage relationships for "active" ion transport systems: I. Steady-state reaction-kinetic analysis of class-I mechanisms. *J. Membrane Biol.* **63:**165–190

Hansen, U.-P., Tittor, J., Gradmann, D. 1983. Interpretation of current-voltage relationships for "active" ion transport systems: II. Nonsteady reaction kinetic analysis of class-I mechanisms with one slow time constant. *J. Membrane Biol.* **75:**141–169

Hayama, T., Shimmen, T., Tazawa, M. 1979. Participation of Ca^{2+} in cessation of cytoplasmic streaming induced by membrane excitation in *characeae* internodal cells. *Protoplasma* **99**:305–321

Hodgkin, A.L., Huxley, A.F. 1952. A quantitative description of membrane current and its application to conduction and excitation in nerve. *J. Physiol. (London)* **117**:500–544

Hope, A.B., Findlay, G.P. 1964. The action potential in *Chara*. *Plant Cell Physiol.* **5**:377–379

Hope, A.B., Walker, N.A. 1975. The Physiology of Giant Algal Cells. Cambridge University Press, London

Keifer, D.W., Spanswick, R.W. 1979. Correlation of adenosine triphosphate levels in *Chara corallina* with the activity of the electrogenic pump. *Plant Physiol.* **64**:165–168

Kikuyama, M., Tazawa, M. 1983. Transient increase of intracellular Ca^{2+} during excitation of tonoplast-free *Chara* cells. *Protoplasma* **117**:62–67

Kishimoto, U. 1964. Current voltage relations in *Nitella*. *Jpn. J. Physiol.* **14**:515–527

Kishimoto, U. 1965. Voltage clamp and internal perfusion studies on *Nitella* internodes. *J. Cell. Comp. Physiol.* **66**:43–53

Kishimoto, U., Kami-ike, N., Takeuchi, Y. 1980. The role of electrogenic pump in *Chara corallina*. *J. Membrane Biol.* **55**:149–156

Kishimoto, U., Kami-ike, N., Takeuchi, Y. 1981. A quantitative expression of the electrogenic pump and its possible role in the excitation of *Chara* internodes. *In:* The Biophysical Approach to Excitable Systems. W.J. Adelman, Jr., and D.E. Goldman, editors. pp. 165–181. Plenum, New York

Kishimoto, U., Kami-ike, N., Takeuchi, Y., Ohkawa, T. 1982. An improved method for determining the ionic conductance and capacitance of the membrane of *Chara corallina*. *Plant Cell Physiol.* **23**:1041–1054

Kishimoto, U., Kami-ike, N., Takeuchi, Y., Ohkawa, T. 1984. A kinetic analysis of the electrogenic pump of *Chara corallina*: I. Inhibition of the pump by DCCD. *J. Membrane Biol.* **80**:175–183

Kitasato, H. 1968. The influence of H^+ on the membrane potential and ion fluxes of *Nitella*. *J. Gen. Physiol.* **52**:60–87

Kotani, T. 1979. A modification of Powell's method for minimization of nonlinear functions. *Computer Center News* (Osaka University) **32**:27–47

Läuger, P. 1979. A channel mechanism for electrogenic ion pumps. *Biochim. Biophys. Acta* **552**:143–161

Läuger, P. 1980. Kinetic properties of ion carriers and channels. *J. Membrane Biol.* **57**:163–178

Mullins, L.J. 1962. Efflux of chloride ions during the action potential of *Nitella*. *Nature (London)* **196**:986–987

Oosawa, F., Hayashi, S. 1983. Coupling between flagellar motor rotation and proton flux in bacteria. *J. Phys. Soc. Jpn.* **52**:4019–4028

Powell, M.J.D. 1965. A method of minimizing a sum of squares of nonlinear functions without calculating derivatives. *Computer J.* **7**:303–307

Smith, F.A. 1984. Regulation of the cytoplasmic pH of *Chara corallina* in the absence of external Ca^{2+}: Its significance in relation to activity and control of the H^+ pump. *J. Exp. Bot.* **35**:1525–1536

Smith, J.R., Beilby, M.J. 1983. Inhibition of electrogenic transport associated with the action potential in *Chara*. *J. Membrane Biol.* **71**:131–140

Spanswick, R.M. 1981. Electrogenic ion pumps. *Annu. Rev. Plant Physiol.* **32**:267–289

Steinmetz, P.R., Andersen, O.S. 1982. Electrogenic proton transport in epithelial membranes. *J. Membrane Biol.* **65**:155–174

Takeuchi, Y., Kishimoto, U. 1983. Changes of adenine nucleotide levels in *Chara* internodes during metabolic inhibition. *Plant Cell Physiol.* **24**:1401–1409

Takeuchi, Y., Kishimoto, U., Ohkawa, T., Kami-ike, N. 1985. A kinetic analysis of the electrogenic pump of *Chara corallina*: II. Dependence of the pump on the external pH. *J. Membrane Biol.* **86**:17–26

Williamson, R.E., Ashley, C.C. 1982. Free Ca^{2+} and cytoplasmic streaming in the alga *Chara*. *Nature (London)* **296**:647–650

Received 17 December 1984; revised 12 March 1985